JOURNAL OF OPTOELECTRONICS AND ADVANCED MATERIALS Vol. 10, No. 1, January 2008, p. 131 - 140

Structural transformations in amorphous As_xSe_{1-X} ($0 \le x \le 0.20$) films

V. I. MIKLA*, V. V. MIKLA[a]
Institute for Solid State Physics and Chemistry, Uzhgorod National University, Uzhgorod, Voloshina 54, Ukraine
[a]Yazaki, Ukraine, Ltd

Structural transformations are examined through Raman scattering measurements for amorphous Se-rich As_xSe_{1-x} ($0 \le x \le 0.2$) alloys. It is found that the molecular structure of amorphous Se (a-Se) on the scale of medium-range order differs from the structure of most inorganic glasses and may be placed between three-dimensional network glasses and polymeric ones. Further experiments show the existence of successive phases in laser-induced glass - crystalline transition with pronounced threshold behavior. By comparing peak width, peak location and Raman intensity in the range of bond modes it is derived that the changes occur not monotonically with increasing As content. The composition-induced changes of the spectra are explained by cross-linking of Se chains. Under laser irradiation, the changes in the optical transmission, holographic recording properties and Raman spectra of amorphous As_xSe_{1-x} films with $0 < x \le 0.2$ have been examined. The dependence of the transmissivity and diffraction efficiency on the irradiation energy density shows two qualitatively different regions. Below the energy density threshold, E_{th}, only small changes in the local structure of the system can be detected. In the low-energy region, transient changes in transmissivity are observed. Qualitative explanation of this behavior may be based on associating such with alternating of deep defect states. Above E_{th}, the changes were attributed to crystallization transformation. The corresponding Raman spectra reveal transformation of the system from amorphous into the crystalline phase under laser irradiation. Although several articles and texts have provided reviews on various properties and applications of chalcogenide glasses, there is no thorough study of local atomic structure and its modification for Se-rich amorphous As_xSe_{1-x}. The present paper is concerned with this problem.

(Received September 25, 2007; accepted January 10, 2008)

Keywords: Amorphous chalcogenides, Raman scattering, Structural transformations

1. Introduction

In recent years there has been enhanced interest in structural studies of chalcogenide glasses owing to their present and potential use in electrical and optical devices. As-containing chalcogenides, especially Se-rich alloys, usually have been studied in thin film, bulk and fiber forms. Since change in the structure can have an influence on photogeneration, charge carriers transport, trapping and other important fundamental properties, knowledge of the molecular structure of such materials is needed for further improvement of their characteristics.

Undoubtedly, elemental semiconductors are useful and suitable model objects for studying the influence of structure on physical properties. This is particularly true in respect of selenium. In the past, the latter was successfully used in photocells, rectifier diodes and solar cells. In its amorphous form, selenium has a good application as photoreceptor in copying machines and X-ray imaging plates [1-5]. It is necessary to note that this material is distinctive from other amorphous chalcogenides in several respects:

(a) selenium is the only which vitrifies as an elemental glass and is fairly stable at room temperature;
(b) compositional (chemical) disorder is absent;
(c) charge carriers of both polarities are mobile at room temperature;
(d) spectral dependence of the optical absorption in the region above the Urbach tail is unusual;
(e) there exists a so-called "non-photoconductive gap";
(f) gap-states density in the mobility gap is relatively low respectively to other amorphous materials, etc.

Despite the increasing commercial using of a-Se in various applications (see [4] and references therein), e.g. as promising X-ray flat panel detectors for medical purposes [2], its structure is not fully understood.

On the other hand, binary non-crystalline semiconductors of As-Se system are also of continued scientific and practical interest because of real opportunity of their technological uses (e.g. as functional elements of multi-layer photoreceptors in xerography). Among them the stoichiometric composition, As_2Se_3, and compositions from the range 30-50 at % As are perhaps the most studied ones [2-4]. As for a most of stable binary glasses in As-Se system, which are also the discussion subject of the present paper, atomic ratios can be varied in a wide range. Although the information about various physical properties of Se-rich alloys is not so extensive and numerous [2,3-7,9,11-13,42], their compositional dependence manifests extrema or thresholds also in the range 6-12 at % As. It is necessary to accentuate that the As-Se amorphous alloy system display main extrema of various properties at the composition where the valence requirements appear to be satisfied that is at the stoichiometric composition. It seems to be reasonable to connect the mentioned non-monotonic behavior with a specific character of local structure changes.

Another prominent feature of the materials studied consists in the following. Certain type of glasses whose common feature is the presence of chalcogen atoms, sulfur, selenium, and tellurium, exhibit various photoinduced phenomena (the reader may refer to Ke.Tanaka [14]). Among these are photostructural transformations and photocrystallization phenomena: a change in optical, electrical and other physical properties are observed. The phase transformation of selenium and its alloys can also be induced relatively simply by laser illumination [2,15-17]. Reasonably, this unique property makes them attractive for optical data storage and holographic recording. Many experimental results using selenium and its alloys have been reported [3], but few cases of phase transformation properties were mentioned.

Raman scattering is a very powerful experimental technique for providing information on the constituent structural units in a given material [18]. In the present paper the Raman scattering in pure amorphous selenium (a-Se) and Se-rich As-Se amorphous films are studied. Below we attempt to clarify the structural transformations induced by light treatment and compositional changes. We focus our attention mainly on photocrystallization transformations, although photostructural changes are also considered. The paper also deals with the composition induced structural modifications in amorphous As_xSe_{1-x}. As shows the analysis of Raman data, some discontinuity of atomic arrangement with rising As content exists.

2. Experimental

The samples used in these studies were amorphous films, about 10 μm thick, prepared by vacuum thermal evaporation of the powdered As_xSe_{1-x} melt-quenched material at the rate of 1 μm/min onto quartz substrates held at room temperature as well as polished mirror-like parallelepipeds of vitreous As_xSe_{1-x}. The As_xSe_{1-x} bulk glasses were prepared according to the conventional melt-quenching method. Annealing of the films was carried out in air at ambient pressure and at temperatures below the glass-transition temperature. Thin film samples were kept in complete darkness until measured to minimize exposure to light sources, which could lead to changes in the properties and structure of the films. It is important accentuate that after annealing procedure their Raman spectra become indistinguishable from the corresponding spectra of melt-quenched glassy samples. It should be noted that for Se-rich compositions studied the difference in the spectra of melt-quenched and as-deposited samples is not so "dramatic" as in the case of As-S system as reported by Nemanich et al. [19] (see also [20]).

Right-angle Raman spectra were measured using RAMANOR U-1000 spectrometer. The spectral slit width was ~1 cm^{-1} and the excitation wavelength 676 nm. Raman spectra of the amorphous films were recorded with sufficiently low incident laser-beam power densities P=3 to 5 mW to avoid photostructural changes. The latter is known to transform the Raman spectra in a manner similar to that reported in [21] for amorphous selenium. The identity of the experimental spectra obtained from different points of the sample and the good reproducibility of the spectra in repeated scans (the time required to scanning one spectrum in the spectral range 100-300 cm^{-1} is about 5 min) show that photodarkening did not play a role in the subsequent Raman measurements.

In the transmission photodarkening experiments, the samples were illuminated at near-normal incidence by argon-ion and helium-neon lasers operating, respectively, at 514 nm and 633 nm. These wavelengths were convenient because they correspond to near maximum photoresponse. The transmission of the sample was probed using a portion of the He-Ne output and detected by a photomultiplier. The intensity of the probe beam was kept low ($P \leq 0.01$ W/cm^2) and had no measurable effect on the sample, either in producing or erasing the photodarkening. The sample transmission was measured at 633 nm, during and after photodarkening.

The structure of photocrystallized films was investigated using X-ray diffraction.

The holographic gratings were recorded on thin-film samples of As_xSe_{1-x}. The present grating technique is the conventional method in which a grating having a pitch $\Lambda = \lambda/[2 \sin(\Theta/2)]$ is produced by two interfering beams of wavelength, λ (633 nm), intersecting at a sample surface with an angle, Θ (~ 40^o). The diffraction efficiency, $\eta = I/I_0$, where I_0 and I are the corresponding intensities of a reading beam and of the first order diffracted beam, is measured as a function of the exposure time.

3. Raman scattering in amorphous selenium

In Fig. 1, a typical Raman spectrum of a-Se measured at low incident radiation power density, ~3 mW, is shown. The stable level of the scattered light intensity and the good reproducibility of the spectrum in the repetitive cycles clearly indicate the absence of any structural changes in a-Se induced by laser irradiation of such power density. On the high-frequency side (ω=100 to 300 cm^{-1}) the spectrum contains an intensive peak at 255 cm^{-1} and some peculiarity (shoulder) at 237 cm^{-1}.

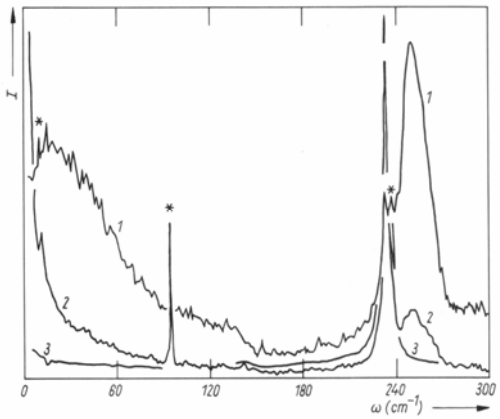

Fig. 1. Raman spectra of (1) amorphous and (2), (3) photocrystallized selenium. Experimental details for (2) and (3) are: (2) after 5 min exposure of the sample to 10 mW, (3) after 30 min exposure to 10 mW . Asterisks indicate laser plasma lines.

The above features are in good agreement with previously reported data [22-25]. In the low-frequency region one can observe the broad peak with ω_{max} = 16 to 20 cm^{-1}. This so-called boson peak occurs in the low frequency region of the Raman spectra of all amorphous and vitreous solids. An analysis of the spectral form of the boson peak is displayed in Fig. 2.

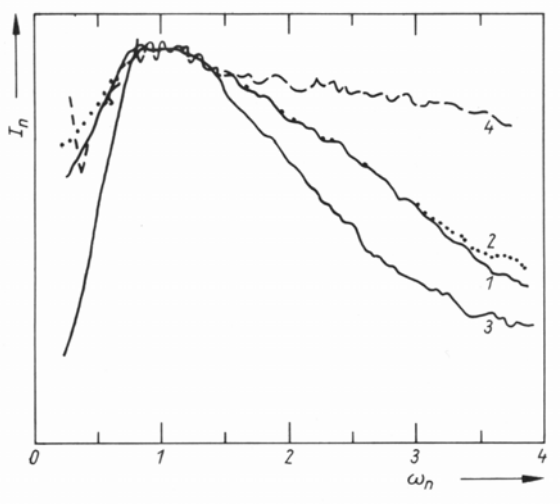

Fig. 2. Low-frequency Raman spectra of different glasses in a scale $\omega_n=\omega/\omega_{max}$. (1) Se ($\omega_{max}$=17 cm^{-1} at T=100 K), (2) Se (ω_{max}=17 cm^{-1} at T=300 K), (3) As_2Se_3 (ω_{max}=26 cm^{-1}, T=300 K [30]), (4) polymethylmetacrylate (PMMA) (ω_{max}=17 cm^{-1} [36]); see also [31-35] for the structural characterization of amorphous chalcogenides).

Normalized Raman spectra $I_n=I/\omega(n(\omega) + 1)$ for a-Se and series of other composition samples are given in the same energy scale $\omega_n=\omega/\omega_{max}$, where $n(\omega) + 1=1/(\exp(h\omega/kT) - 1) + 1$ is the boson factor for the Stokes component.

When we try to identify certain vibration bands observed in the Raman spectrum of a-Se, some difficulties arise. Initially it was proposed to interpret the a-Se Raman spectrum by analogy with sulfur – on the basis of a molecular approach. That is, the main vibration band was considered to be the superposition of the peaks at 237 and 255 cm^{-1} characteristic of chains and rings, respectively [23]. However, further experimental data have caused some doubts to be cast. In such a case one would expect to observe a discernible difference in the contributions of 237 and 255 cm^{-1} modes to the main vibration band in the samples prepared at different conditions (e.g. substrate temperature during deposition for amorphous films or quenching rate for glassy samples). This may be caused by changes in rings to chains ratio. Therefore, it is clear that the spectral region 200 to 300 cm^{-1} is unsuitable for ring diagnostics. This is consistent with the conclusions of [24].

The Se_8 peak (112 cm^{-1}) could not be detected in the present experiment. Probably, this is connected with its weakness. This fact indicates evidently the low concentration of rings. Consequently, one can associate the spectral features in the main vibration band, the 255 cm^{-1} peak and the shoulder at 237 cm^{-1}, mainly with the chain vibrations.

The low frequency region $0 < \omega < 100$ cm^{-1}, in which the boson peak appears, is of special interest. Note that such a low frequency peak seems to be universal feature of all amorphous materials [29,30]. It has been found that the spectral form of the boson peak is the same for a wide series of oxides, chalcogenides, and low-molecular organic glasses and coincides with that of As_2S_3 bulk glass [18,19,30]. The universal form of the low frequency peak is due to universality of glassy material in the scale of medium-range order $L \sim v/\omega_{max}$=1 to 2 nm (v is the sound velocity) [29]. For the case of a-Se, it is observed (Fig. 2) that the spectral form of the boson peak essentially differs from that characteristic of the majority of inorganic glasses. The spectral form of the boson peak in a-Se seems to be intermediate between that in polymeric and low-molecular glasses.

This result can be explained by a preferentially chain-like structure of a-Se. The latter may form a structure similar to the structure of linear polymers PMMA. In other words, with regard to its structure on the scale of medium-range order, a-Se may be placed between 3-dimensional network glasses and polymeric ones. Examples of mediate-range order in elemental and compound materials, including a-Se, have been extensively discussed in [21,27-30].

There exists another possible explanation. Se has its glass transition temperature near room temperature, therefore it is in a well annealed state. It is known [29] that the intensity of the boson peak relative to the main bond modes in the Raman spectrum significantly decreases as the structural order of the sample increases (e.g. in "equilibrated" or annealed samples). This decrease in turn may lead, respectively, to an increased contribution from other modes to the high-frequency side ($\omega \ge \omega_{max}$) of the boson peak. This is clearly seen if we compare the shape of corresponding peaks in a-Se and As_2S_3 (Fig. 2).

4. Composition dependence of Raman bands in amorphous Se-rich alloys As_xSe_{1-x}

In the present section experimental results on Raman scattering spectra for Se-rich amorphous semiconductors As_xSe_{1-x} are discussed. In Fig. 3 typical Raman spectra of amorphous Se and As-Se alloys with As content up to 5 at % are shown. The major spectral feature in the high-frequency region is the 255 cm^{-1} band. Another prominent spectral feature which is not shown in this Figure is the broad peak at ω_{max}=16÷20 cm^{-1}. As mentioned, the latter is characteristic for Raman scattering of all amorphous solids and glasses.

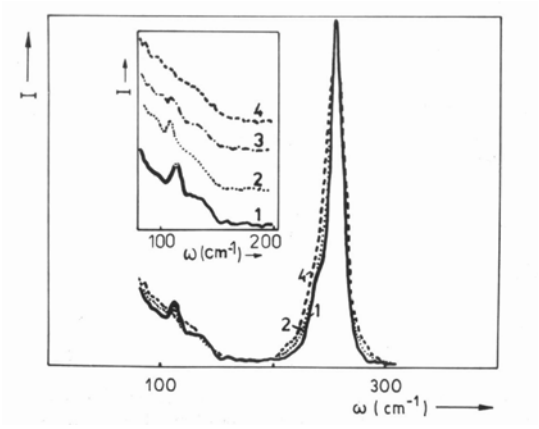

Fig. 3. Comparison of the Raman spectra of (1) amorphous Se and As_xSe_{1-x}: (2) x=0.02, (3) 0.04, and (4) 0.05 at %. Each trace has been normalized to the same peak (255 cm^{-1}) intensity. The inset shows the bending mode region.

In the following we consider only the high-frequency region. The weak feature observed at 112 cm^{-1} in the a-Se spectrum diminishes with As addition and at 5 at % completely disappears (see inset Fig. 3). At the same time the difference in the spectra in the region of the main vibration band is obvious. Thus, with increase of As content the transformation of the Raman spectrum in this region is retraced (Fig. 4).

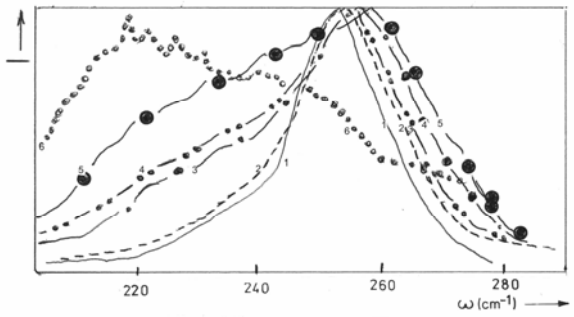

Fig. 4. Raman spectra of amorphous As_xSe_{1-x} films. (1) x=0 (solid line), (2) 0.05 (dashed line), (3) 0.10 (dashed-doted line), (4) 0.12 (dashed-double doted), (5) 0.20 (solid circles), and (6) 0.40 (points). We have used this unconventional denotions for Raman spectra to be distinguishable.

The most important points are the following.
1. Spectrum broadening with increasing As addition.
2. Growth of scattered light intensity from the low-frequency side of the main maximum (255 cm^{-1}).
3. Appearance of a broadened band at 220÷230 cm^{-1} (this band is the most intense in the Raman spectrum of $As_{0.4}Se_{0.6}$). It should be noted also that the main maximum is slightly shifted to higher frequency for amorphous As_xSe_{1-x} respectively to Se (255cm^{-1}).

The intensity of the 220÷230 cm^{-1} band in the As concentration interval 0-5 at % remains practically unchanged. Then, at 6 at % As, an increase of the band intensity occurs. A gradual intensity rise is observed for the band at 220 cm^{-1} as the As content is further increased. For As content exceeding 35 at % the band dominates in the Raman spectrum. It seems to be reasonable to approximate the observed Raman spectra of As_xSe_{1-x} as superposition of the spectra of amorphous Se and $As_{0.4}Se_{0.6}$. The corresponding calculations have been performed. These calculations yield that a systematic discrepancy between approximated and experimental spectra is observed. As for the latter, the greater values of the main peak width are typical. Fig. 5 shows difference spectra obtained by subtracting the $As_{0.4}Se_{0.6}$ spectrum from experimental Raman spectra. The relative contribution of the $As_{0.4}Se_{0.6}$ spectrum was fitted to the ~230 cm^{-1} region where the contribution from pure Se was negligibly small. It is obvious that after such a procedure some peak remains, width and position of which differs from that for a-Se. Based on the data given in Fig. 5, values of the parameter A were estimated. This parameter represents the ratio of the integrated Raman intensity in the interval limited by the typical frequencies of $AsSe_{3/2}$ unit vibrations (205 to 230 cm^{-1}) to the integrated intensity of the whole spectrum of valence vibrations: $A = \int_{205cm^{-1}}^{230cm^{-1}} I \Big/ \int_{205cm^{-1}}^{290cm^{-1}} I$ (here I is the intensity of the corresponding Raman band). Fig. 7 shows that the dependence A ~ f(x) is non-monotonous – parameter A increases around ~ 6 at % As. For the frequency range 240 to 270 cm^{-1} the change of scattered intensity with composition has a smoother character. On the same figure, the dependence of the peak frequency, ω_{max}, and its width, $\Delta\omega_{max}$, on As content for the corresponding spectra is displayed. It is important to note the similarity of the composition dependence of A, ω_{max}, and $\Delta\omega_{max}$.

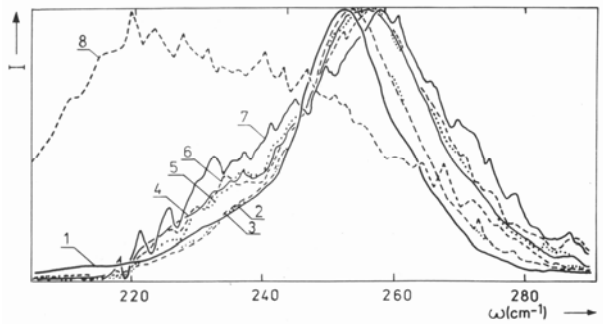

Fig. 5. The difference spectra (for details see the text) for a-As_xSe_{1-x}. x=0.04, 0.05, 0.06, 0.08, 0.10, and 0.20 at %, curves 2 to 7, respectively. For the sake of comparison Raman spectra (1) of a-Se and (8) $As_{0.4}Se_{0.6}$ are also shown.

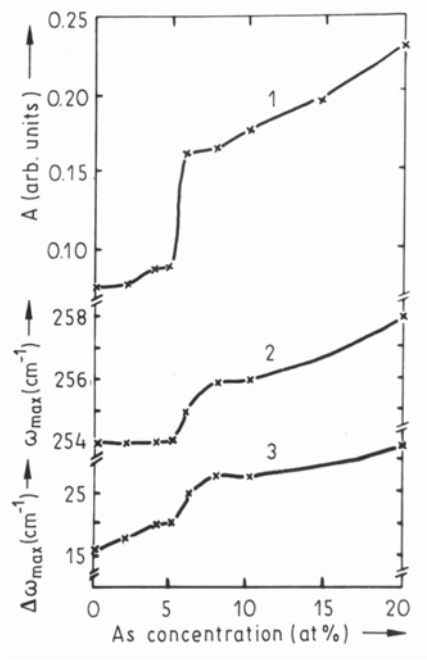

Fig. 6. Composition dependence of the parameters (1) A, (2) ω_{max}, and (3) $\Delta\omega_{max}$.

An attempt to simulate As_xSe_{1-x} Raman spectra by a superposition of two constant spectral forms one of which belongs to a-Se, the other to $As_{0.4}Se_{0.6}$ failed. Onari et al. [37,38] was first who used a similar approach. On the contrary, the experimental spectra could be approximated assuming a considerable broadening of chain vibrations and their frequency displacements. We consider that such an approach is correct and that the difference spectra themselves are convincing arguments in favor of it: the change of the Raman spectra with composition together with parameters A, $\omega_{max,}$, and $\Delta\omega_{max}$ (see the corresponding figures) support this suggestion.

Composition-dependent studies on the physical properties of binary and ternary chalcogenide glasses give evidence for the existence of mechanical and chemical thresholds at certain compositions of these materials [39-41]. The As-Se system displays main extrema of various properties at the stoichiometric composition (the mechanical and chemical thresholds coincides at $x = 0.40$). There seem to exist (see experimental results published by Kasap [42] and present data) an additional threshold at $0.06 \leq x \leq 0.12$. It can be argued that the non-monotonic behavior observed in the concentration dependence of glass transition temperature, density, etc [6] in this range originates from changes in bond topology [40,43]. We assume that in Se-rich glasses the network is dominated by Se atom chains (quasi-one-dimensional network) and addition of As atoms lead to branching owing to threefold coordination of As atoms. Recent publications [42,47,48], as we believe, give a new approach to the problem of local bonding in amorphous chalcogenides. The anomalous behavior near $x \approx 0.06$ is ascribed to the disappearance of Se_8-like segments. From the point of view of configuration, it is suggested that the number of *cis*-configurations starts to decrease, so that the mediate-range correlation is modified. The considerable reduction in the vibration mode at ~112 cm^{-1}, which is associated with *cis*-segments, strongly supports this suggestion. Changes in the Raman spectrum with composition allow us to conclude that incorporation of As leads to cross-links between chain-like or ring-like segments of amorphous Se.

There are strong indications that the compositional dependence of physical and chemical properties has no connection with chemical ordering. In fact, the binary As_xSe_{1-x} alloys exhibit extrema in compositional dependence of the density not only at the $As_{0.4}Se_{0.6}$ composition, but also for the non-stoichiometric chalcogen-rich $As_{0.06}Se_{0.94}$ and also for pnictogen-rich $As_{0.6}Se_{0.4}$ samples. This means that the x dependence of the density originates from changes in bonding topology.

5. Laser-induced structural transformation of As_xSe_{1-x} amorphous films

The photodarkening phenomenon continues to attract extensive interest, since this is a simple, at first sight, bulk phenomenon, which is characteristic of chalcogenide glasses. That is, it does not appear in the corresponding crystal. Although photodarkening and related changes have been extensively studied, the mechanism of this unique phenomenon is not yet elucidated. Fig. 7 illustrates the development of the photodarkening effect (i.e., the change in transmissivity) at room temperature as a function of time with the illumination turned on and off.

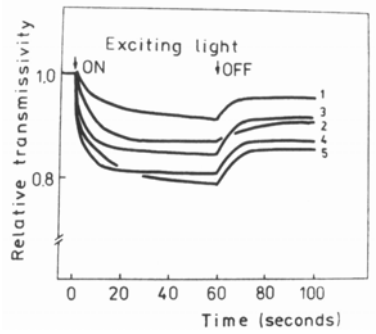

Fig. 7. Time dependence of photo-induced changes in transmissivity in As_xSe_{1-x} films. x=0, 0.02, 0.05, 0.08 and 0.12 in curves 1-5, respectively.

During on-periods, the intensity of illumination remained constant. All As_xSe_{1-x} ($0 \leq x \leq 0.2$) films show a decrease in transmissivity, T_{rel} (i.e., in the ratio between the transmissivity, T_{ir}, of irradiated As_xSe_{1-x} films and the transmissivity, T_u, of untreated films), with the irradiation time. On illumination there is an initial decrease with illumination time up to the constant value. For this rapid change to be observed, an exposure of 10 J/cm^2 is required. The degree of change increases with As content. When the illumination is interrupted, the transmissivity increases (bleaching). The magnitude of bleaching

decreases with addition of As. It is necessary to note that amorphous Se and As_xSe_{1-x} ($0 < x < 0.20$) exhibit appreciable self-annealing effects if photostructural changes are induced near room temperature [14,34,43-46]. The reason for this is that the glass transition temperatures (T_g = 41 and 57 °C for Se and $As_{0.05}Se_{0.95}$, respectively [6]) are close to the illumination temperature. A similar transient transmission change was observed for all samples, irrespective of their composition, previous treatment such as illumination or annealing in dark. These changes in transmissivity in cycles of on-off illumination can be repeated reproducibly many times. In that sense we consider them reversible. These reversible changes appear to saturate after ~ 100 J/cm^2 integrated exposure at exciting light intensities < 0.5 W/cm^2.

Increasing exposure (in our case for intensities > 0.6 W/cm^2) caused a significant irreversible change in transmissivity, which we attribute to a crystallization transformation as discussed below.

After an initial response corresponding to the transient transmission change, there is a slowly varying response. The results, reflecting this situation, are shown in Fig. 8. The slowly varying portion of the darkening curve is followed by a decrease in transmission. The latter appear to indicate actual crystallization (see the corresponding Raman data). The transmission change completed by a saturation region. The latter shows dependence on the intensity of the light.

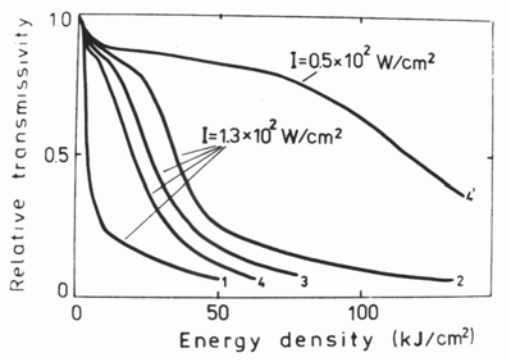

Fig. 8. Evolution of the relative transmissivity change in As_xSe_{1-x} samples exposed to laser illumination at 633 nm. Thickness is 1.2 μm and intensity 1.3×10^2 W/cm^2. x=0, 0.05, 0.08 and 0.12 (curves 1-4, respectively). For a-$As_{0.12}Se_{0.88}$, the corresponding curve is also shown for lower intensity (0.5×10^2 W/cm^2).

The total change in transmission may attain ~90% at such an exposure. The addition of arsenic to amorphous selenium and/or decreasing the temperature (Fig. 9) delays the crystallization onset, which starts at higher exposure times. It is necessary to note that during laser exposure oxidation of films may take place. In Raman spectra of As_xSe_{1-x} samples characteristic to this composition bands are only present. As we believe, this is a strong argument that oxidation may be ruled out in our a case.

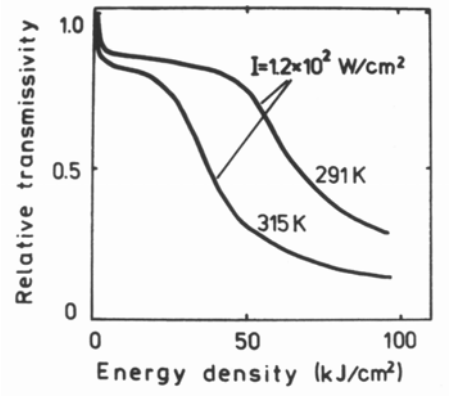

Fig. 9. Change in the relative transmissivity in $As_{0.05}Se_{0.95}$ samples induced by laser irradiation at 291 and 315 K. Inducing intensity was 1.2×10^2 W/cm^2.

When a sample of amorphous selenium is exposed to the 490 nm light (I~1.9 W/cm^2), the transmission characteristics are similar to those induced by 633 nm light. This similarity is the case for all compositions under examination. The observed transient transmission change is ~ 8 %. At the same time we cannot induce crystallization-related effects even for total exposure of 10^4 J/cm^2 at 10^2 W/cm^2.

The holographic gratings were recorded on Se and As_xSe_{1-x} thin films. Fig. 10 shows typical response of light intensities diffracted from gratings formed on As_xSe_{1-x} film. The low-energy region we attributed to transient effects, while the high-energy region is reasonably connected to photocrystallization-related permanent changes.

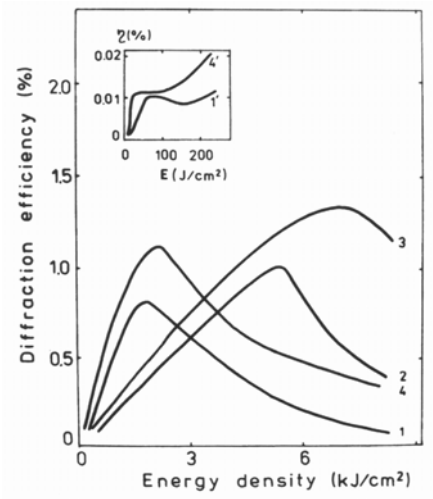

Fig. 10. Diffraction efficiency, η, as a function of energy density for a-As_xSe_{1-x}. x=0, 0.05, 0.08 and 0.12 (curves 1-4, respectively). The inset shows the low-energy region for a-Se (1') and a-$As_{0.12}Se_{0.88}$ (4'). I=0.6 W/cm^2.

The tail observed after η reached maximum at higher exposure is due to the fact that photocrystallization increases the optical absorption for the probing light.

The light scattering spectra recorded after irradiation with an intense laser beam (the exposure conditions were chosen identical to those that cause the above described transmission change) reveal well-defined changes in the structural organization of the films.

We may summarize the general features of the observed transformation of Raman spectra in the range of bond bands for amorphous selenium. 1) There is (Fig. 11) a certain threshold energy, E_{th}, of the incident radiation. 2) Below E_{th}, no changes of Raman spectrum are observed. Here we note that the only exception is the so-called boson peak detected at around 17 cm^{-1} which is weakened by illumination. 3) Above E_{th}, an increase of the incident energy density modifies the spectra.

The present experimental results permit to distinguish three successive stages of photocrystallization in a-Se with regard to irradiation energy density. First of all it is necessary to point out the absence of any significant structural transformations in films and bulk samples at $E_{th} \le 4$ J/cm^2. This is strongly supported by the identity of the Raman spectra recorded in repetitive cycles. At the first stage, which is induced by irradiation with incident energy density ≥ 3.8 J/cm^2, microcrystallite formation probably takes place. In such a case the 255 cm^{-1} peaks dominates the Raman spectra.

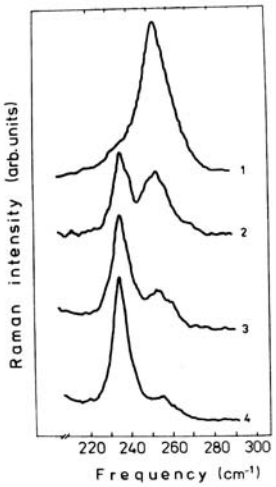

Fig. 11. Laser-induced transformation of Raman spectra of amorphous Se. Experimental details for (1)-(4) are: (1) reference spectrum of amorphous state, (2)-(4) after exposure to E = 3.8, 11,4 and 19 × 10^3 J/cm^2, respectively. I = 1.3 × 10^2 W/cm^2.

The second stage of photocrystallization (~ 11 J/cm^2) is characterized by an enlargement of microcrystalline units. This is demonstrated by the growth of the 237 cm^{-1} peak. Finally, at ~ 20 J/cm^2, photocrystallization practically takes place. This stage is marked by a dramatic increase and narrowing of the peak at 237 cm^{-1} with irradiation time. At the same time, the 255 cm^{-1} peak becomes more and more suppressed with respect to other Raman active modes and, finally, it completely disappears. At this last stage of photocrystallization the absence of the low frequency (17 cm^{-1}) peak is also characteristic.

It seems to be reasonable to assume a thermal, caused by laser heating of the sample, mechanism for the observed structural transformation. This suggestion is strongly confirmed by the clearly manifested threshold behavior. Additional support comes from the fact that at low temperature the threshold power (e.g. 20 J/cm^2 at T=100 K for a-Se) which is necessary for changes in Raman spectra to be observable exceeds several times that for changes at T=300 K. Note that the changes under examination qualitatively differ from the well-known photodarkening phenomena. As for the latter, it takes place at any value of irradiation power; threshold behavior was not characteristic of them. The magnitude of photodarkening depends mainly on the amount of absorbed energy and significantly increases with temperature lowering.

The relatively greater efficiency in films in comparison with bulk samples is established feature of photodarkening. In contrast, in our case, the threshold power densities for a-Se films are found to be higher than for bulk samples. According to results [34,35], discernible, reversible photodarkening in a-Se at T=100 K occurs at photon energy hν ≥2.0 eV with efficiency maximum at ~2.4 eV. Probably, the exciting irradiation energy, hν=1.84 eV seems to be low to induce significant photodarkening at T=100 K. At the same time the probability of transient photodarkening effects relaxing after finishing the irradiation at T=300 K for E ≈ 3.8 J/cm^2 cannot be definitively ruled out.

With regard to As_xSe_{1-x} Raman data, principal results are the following.

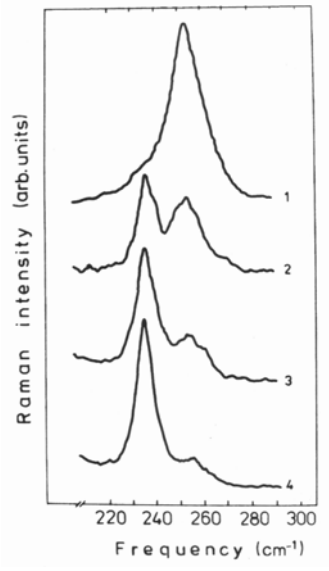

Fig. 12 Development of the photocrystallization effect in $As_{0.05}Se_{0.95}$ as a function of exposure: 1, reference spectrum of amorphous state; 2, 3, after exposure to 15 and 25×10^3 J/cm^2, respectively. I = 1.3 × 10^2 W/cm^2.

(1) The spectra of the As_xSe_{1-x} amorphous alloy samples before irradiation were the same as those reported in Refs [9,19,22,24-25,37-38,46].
(2) The value of E_{th} necessary for changes in Raman spectra to be observable vary with addition of As (see Table 1 given below).

Table 1.

E_{th} values as a function of As concentration in As_xSe_{1-x} alloys

As concentration (at %):	0	5	8	12	20
E_{th}^* (kJ/cm^2):		2±1	12±3	7±2	8±2	45±5

* The E_{th} values are shown for the case $I=1.3\times10^2$ W/cm^2

(3) Under irradiation with $E>E_{th}$ the recorded spectra clearly show a narrowing and increase in the intensity of the 237 cm^{-1} Raman band.
(4) In As_xSe_{1-x} samples with $x\leq0.05$, no additional (to that recorded for pure Se) photoinduced changes in their Raman spectra are observed (see Fig. 12 and compare with the results for a-Se). It should be accentuated that, on introducing such a relatively large quantity of As additives, there is no appreciable influence on the photocrystallization product.
It is well known that Se is likely to be photocrystallized at ~350 K [6,15]. Reasonably, X-ray diffraction patterns of the samples have been measured. Since the illumination region is of ~3mm in radius, the pattern is noisy. However, we can clearly see four crystalline peaks located at 2θ = 24°, 30°, 41°, and 45°. The peaks can be indexed, respectively, as 100, 101, 110, and 111 of the trigonal (hexagonal) Se crystal [59].
(5) For As content >15 at%, the main result of this study is the appearance and disappearance of new Raman bands typical for $As_{0.4}Se_{0.6}$.

For example, Fig. 12 shows the appearance of an additional peak (~264 cm^{-1}) superimposed on the amorphous peak (~255 cm^{-1}). With a further increase of the irradiation energy density, crystallization starts immediately. Here we should note an evolution qualitatively similar to that shown for pure Se and $As_{0.05}Se_{0.95}$ in the shape of spectra over the concentration range 0-20 at %. In the final stage of photocrystallization, the spectra of As_xSe_{1-x} alloys are free of key crystalline features that occur [52] in the spectra of crystalline As_2Se_3. It is of particular significance that only the 237 cm^{-1} band of trigonal selenium contributes to the spectra of photocrystallized As_xSe_{1-x} ($0<x<20$) films.

In order to discuss further the changes in the optical transmissivity and diffraction efficiency with irradiation energy density, we will divide the T_{rel} and η versus E data into two qualitatively different regions with a separation at E_{th}. We define E_{th} (e.g. $E_{th}=2\times10^3$ J/cm^2 at $I=1.3\times10^2$ W/cm^2 in the case of pure Se) as the energy density for which the system is not yet perturbed structurally (on the scale of short-range order) by laser irradiation. The absence of any significant bonding changes in films is supported by the identity of the Raman spectra recorded in repetitive cycles. This result holds for both pure amorphous selenium and Se-rich As_xSe_{1-x} alloys. For energies less than E_{th} reversible photodarkening and transient transmission changes are observed. These effects are characteristic of the amorphous phase and the system remains in the amorphous phase under or even after irradiation. The lack of any noticeable variation in the transient behavior T_{rel} for samples of different substrate material and film thickness exclude the possibility of the effect being due to small changes in sample temperature during and after illumination, i.e., to photoinduced heating.

We have recently reported similar dynamical photoinduced changes in some photoelectronic properties detected by time-of-flight and xerographic technique [43,54]. These experiments may provide the first evidence that deep defects can be altered temporarily by room-temperature irradiation. Note that there is a close correlation between the recovery of optical parameters and photoelectronic characteristics in exposed samples. Although a complete correlation of microscopic structural modifications with macroscopic photodarkening phenomena must await further experimental measurements, it is only natural that we relate the transient changes in the transmissivity with changes in deep defect states. We identify such centers as arising from native (thermodynamic) structural defects (e.g., C_3^+ and C_1^- in amorphous selenium). Band-gap light can probably initiate conversion of traps of small cross-section to those of larger cross-section [3,28].

By contrast, above E_{th}, all the observed irreversible changes may be attributed to optical constant variations and modifications in the kinetics of light-induced crystallization. The present experimental results resolve successive stages of photocrystallization in a-Se (these were mentioned above). In such a photocrystallization process, amorphous Se undergoes a transformation to the trigonal selenium which is the most stable modification. Raman scattering studies together with X-ray diffraction data gave an unambiguous indication of trigonal selenium.

On the basis of the present Raman data, we conclude that the features of the photocrystallization effects in As_xSe_{1-x} alloys with $x<0.15$ are qualitatively the same as those in amorphous selenium. Some deviation in pre-crystallization behavior of $As_{0.2}Se_{0.8}$, namely the appearance and disappearance of the weak quasi-crystalline peak at 264 cm^{-1}, probably indicates As_2Se_3-like cluster creation and annihilation. The latter could be clusters with a more ordered structure with respect to that existing in amorphous phase. At the same time, they are not yet microcrystallites with inherent Raman peaks. It seems to be reasonable that the environment of the clusters prevents their growth and transformation into microcrystallites. Other Se clusters reach the critical size required for microcrystallite formation. After that, sample exposure to $E>E_{th}$ crystallized selenium, while the As-containing clusters remained in amorphous phase. The above explanation is in agreement with the results of the study of laser-induced structural transformations in glassy As_2Se_3 [28] and also with the mechanism proposed by Phillips [56].

It is known [6] that As is an effective additive to decrease the tendency to crystallization. Our experimental results, namely the greater value of E_{th} for a-As_xSe_{1-x} films, indicate that the addition of As effects the suppression of the crystal nucleation and growth in amorphous selenium. The long Se chains in amorphous selenium branch at the site of As atoms. The length of Se chains becomes short [38,46] and the amorphous Se cannot easily crystallize with increase of As concentration.

At the same time, it is necessary to note that the changes in optical transmissivity and diffraction efficiency that occur are not monotonic with increasing As content. It seems to be reasonable to connect such a behavior with some discontinuity of atomic arrangement with increasing As content. Our recent study of composition dependence of Raman bands in amorphous As_xSe_{1-x} supports this suggestion.

6. Conclusions

The molecular structure of amorphous selenium differs from the that of the majority of inorganic glasses on a scale of medium-range order. Apparently, Se chains form a structure similar to the structure of linear polymers on the scale ~1 nm. The dependence of the transmissivity and diffraction efficiency on the irradiation energy density shows two qualitatively different regions. Below the energy density threshold, E_{th}, only small changes in the local structure of the system can be detected. In the low-energy region, the transmissivity varies reversibly (transient changes) with exposure. Qualitative explanation of the observed behavior may be based on associating such with alternating of deep defect states. Above E_{th}, the changes were attributed to crystallization transformation. In addition, we have detected the successive phases in such a transition which is a threshold phenomenon.

It has been shown that Raman scattering spectra of amorphous As_xSe_{1-x} alloys change non-monotonically with composition in the region of bond stretching modes. Certain extrema in various physical properties exist at composition range 6-12 at % As. The presence of this topological threshold is established by direct evidence, such as peculiarities in the compositional dependence of the Raman vibration modes of glasses. These peculiarities are caused by the transition from a chain-ring-like structure to chainlike structure with increasing degree of cross-linking.

By correlating the changes observed in optical properties under increasing irradiation energy density with insights into molecular structure gained from Raman scattering studies, we have shown how the structure transforms chronologically in amorphous As_xSe_{1-x} recording media.

Laser-induced optical changes at room temperature involve two phenomena essentially different in their origin: transient reversible changes (photodarkening) and irreversible changes (photocrystallization) with gross structural reorganization. For high values of energy density, the Raman spectrum has pronounced crystallization-related changes.

Our explanation are based on the assumption that the radiation pumps the material from an amorphous state towards the crystalline state through the formation of small clusters, which coalesce to form large clusters attaining microcrystallite size at high energy density levels.

References

[1] A. Madan, M. P. Shaw, "The Physics and Applications of Amorphous Semiconductors" (Academic Press, Boston, MA, 1988).

[2] A. Feltz, "Amorphous Inorganic Materials and Glasses" (VCH, Weinheim, Germany 1993).

[3] S. O. Kasap, in "Handbook of Imaging Materials" edited by A. S. Diamond and D. S. Weiss (Marcel Dekker, Inc., New York, Second Edition, 2002) p. 329, and references therein.

[4] K. Tanaka, in "Encyclopedia of Materials (Elsevier Science Ltd., 2001) p. 1123.

[5] S. O. Kasap, J. A. Rowlands, J. Mater. Sci. Mater. Electron. **11**, 179 (2000).

[6] Z. Borisova, "Glassy Semiconductors" (Plenum Press, New York, 1981).

[7] N. F. Mott, E. A. Davis, "Electronic Processes in Non-Crystalline Naterials" (Oxford University Press, Oxford, Second Edition, 1979).

[8] K. Hulls, P. W. Mc Millan, J. Non-Cryst. Solids **15**, 357 (1974).

[9] J. Schottmiller, M. Tabak, G. Lucovsky, A. Ward, J. Non-Cryst. Solids **4**, 80 (1970).

[10] A. E. Owen, A. P. Firth, P. J. S. Ewen, Philos. Mag. **B 52**, 347 (1985).

[11] A. E. Owen, W. E. Spear, Phys. Chem. Glasses **17**, 174 (1976).

[12] V. I. Mikla, D. G. Semak, A. V. Mateleshko, A. R. Levkulich, Sov. Phys. Semicond. **21**, 266 (1987).

[13] V. I. Mikla, D. G. Semak, A. V. Mateleshko, A. R. Levkulich, Sov. Phys. Semicond. **23**, 80 (1989).

[14] K. Tanaka, Rev. Solid State Sci. **2&3**, 644 (1990).

[15] J. Dresner, G. B. Strinfellow, J. Phys. Chem. Solids **29**, 303 (1968).

[16] J. P. De Neufville, in "Optical Properties of Solids – New Developments" edited by D. O. Seraphin (North-Holand, Amsterdam, 1975) p. 437.

[17] H. Fritzsche, in "Insulating and Semiconducting glasses" edited by P. Boolchand (World Scientific, Singapore,2000) Chap 10.

[18] M. Cardona, "Light Scattering in Solids" (Springer-Verlag, Berlin, 1975).

[19] R. J. Nemanich,G. A. Connell, T. M. Hayes, R. A. Street, Phys. Rev. B **18**, 6900 (1978).

[20] V. I. Mikla (PhD Thesis, Odessa State university, Odessa, 1984).

[21] A. A. Baganich, V. I. Mikla, D. G. Semak, A. P. Sokolov, Phys. Stat. Sol. (b) **166**, 297 (1991).

[22] M. Gorman, S. A. Solin, Solid State Commun. **18**, 1401 (1976).

[23] M. H. Brodsky, M. Cardona, J. Non-Cryst. Solids **31**, 81 (1978).

[24] P. J. Carroll, J. S. Lannin, Solid State Commun. **40**,

81 (1981).
[25] P. J. Carroll, J. S. Lannin, J. Non-Cryst. Solids **35/36**, 1277 (1980).
[26] G. Lucovsky, F. L. Galeneer, J. Non-Cryst. Solids **35/36**, 1209 (1980).
[27] J. Jakle, in: Amorphous Solids: Low-Temperature Properties, Ed. W. A. Phillips, (Springer-Verlag, Berlin, 1981), p. 135.
[28] V. I. Mikla, Dr. Sci. Thesis, Institute of Solid State Physics, (Academy of Sciences, Kiev, 1984).
[29] V. K. Malinovsky, V. N. Novikov, V. P. Sokolov, Phys. I Khim. Stekla, **15**, 331 (1989).
[30] V. K. Malinovsky, V. P. Sokolov, Solid State Commun. **57**, 757 (1986).
[31] G. Lucovsky, J. Non-Cryst. Solids **97/98**, 155 (1987).
[32] H. Richter, Z. P. Wang, L. Ley, Solid State Commun. **39**, 625 (1981).
[33] V. M. Lyubin, in: Non-Silver Photographic Processes, (Khimiyia, Leningrad, 1984).
[34] K. Tanaka, N. Odajima, Solid State Commun. **43**, 961 (1982).
[35] R. T. Phillips, J. Non-Cryst. Solids **70**, 359 (1985).
[36] V. A. Bagrynskii, V. K. Malinovsky, V. N. Novikov, L. M. Puschaeva, A. P. Sokolov, Fiz. Tverd. Tela **30,** 2360 (1988).
[37] T. Mori, S. Onari, T. Arai, J. Appl. Phys. **19**, 1027 (1980).
[38] S. Onari, K. Matsuishi, T. Arai, J. Non-Crystall. Solids **74,** 57 (1985).
[38] J. C. Phillips, J. Non-Cryst. Solids **43**, 37 (1981).
[39] M. F. Thorpe, J. Non-Cryst. Solids **57**, 355 (1983).
[40] K. Tanaka, Phys. Rev. B **39**, 1270 (1989).
[41] T. Wagner, S. O. Kasap, Phil. Mag. B **74**, 667 (1996).
[42] V. I. Mikla, J. Phys.: Condes. Matter **9**, 9209 (1997).
[43] V. L. Averianov, A. V. Kolobov, B. T. Kolomiets, V. M. Lyubin, Phys. Stat. Solidi (a) **57,** 81 (1980).
[44] K. Tanaka, A. Odajima, Solid State Commun. **43,** 961 (1982).
[45] V. I. Mikla, D. G. Semak, A. V. Mateleshko, A. A. Baganich, Phys. Stat. Solidi (a) **117,** 241 (1990).
[46] P. Boolchand, M. Jin, D. I. Novita, S. Chakravarty, J. Raman Spectroscopy (2007) (in press).
[47] E. Ahn, G. A. Williams, P. C. Taylor, Phys. Rev. B **74**, 174206 (2006).
[48] V. L. Averianov, A. V. Kolobov, B. T. Kolomiets, V. M. Lyubin, Phys. Stat. Solidi (a) **57,** 81 (1980).
[49] V. I. Mikla, I. P. Mikhalko, J. Non-Cryst. Solids **180,** 236 (1995).
[50] M. Chomat, D. Lezal, J. Gregore, I. Srb, J. Non-Crystall. Solids **20,** 427 (1976).
[51] R. Zallen, M. L. Slade, A. T. Ward, Phys. Rev. **B3,** 4257 (1971).
[52] M. Abkowitz, R. C. Enck, Phys. Rev. **B25,** 2567 (1982).
[53] M. Abkowitz, R. C. Enck, Phys. Rev. **B27,** 7402 (1983).
[54] I. Abdulhalim, R. Besserman, Solid State Commun. **64,** 951 (1987).
[55] J. C. Phillips, Solid State Phys. **10,** 165 (1982).
[56] Yang Hanmei, Wang Weizhong, Min Szukwei, J. Non-Cryst. Solids **80,** 503 (1986).
[57] J. Dresner, G. B. Strinfellow, J. Phys. Chem. Solids **29**, 303 (1968).
[58] Powder Diffraction File (ASTM card), ed. L. G. Berry (Joint Committie on Powder Diffraction Standard, Philadelphia, 1974).

*Corresponding author: mikla_v@ukr.net